REPORT SD-TR-80-65

LEVEL II

Microcracking in Graphite-Epoxy Composites

E. G. WOLFF
Materials Sciences Laboratory
Laboratory Operations
The Aerospace Corporation
El Segundo, Calif. 90245

1 September 1980

Interim Report

THE AEROSPACE CORPORATION
Prepared for
SPACE DIVISION
AIR FORCE SYSTEMS COMMAND
Los Angeles Air Force Station
P.O. Box 92960, Worldway Postal Center
Los Angeles, Calif. 90009

This interim report was submitted by The Aerospace Corporation, El Segundo, Calif. 90245, under Contract No. F04701-79-C-0080 with the Space Division, Contracts Management Office, P.O. Box 92960, Worldway Postal Center, Los Angeles, Calif. 90009. It was reviewed and approved for The Aerospace Corporation by W. C. Riley, Director, Materials Sciences Laboratory. Gerhard E. Aichinger was the project officer for Mission-Oriented Investigation and Experimentation (MOIE) Programs.

This report has been reviewed by the Information Office (OI) and is releasable to the National Technical Information Service (NTIS). At NTIS, it will be available to the general public, including foreign nations.

This technical report has been reviewed and is approved for publication. Publication of this report does not constitute Air Force approval of the report's findings or conclusions. It is published only for the exchange and stimulation of ideas.

Gerhard E. Aichinger
Project Officer

FOR THE COMMANDER

EVAN R. BROSSMAN
Chief, Contracts Management Office

UNCLASSIFIED

SECURITY CLASSIFICATION OF THIS PAGE (When Data Entered)

REPORT DOCUMENTATION PAGE

READ INSTRUCTIONS BEFORE COMPLETING FORM

1. REPORT NUMBER: SD-TR-80-65	2. GOVT ACCESSION NO.: AD-A089 894
3. RECIPIENT'S CATALOG NUMBER:	
4. TITLE (and Subtitle): MICROCRACKING IN GRAPHITE-EPOXY COMPOSITES.	5. TYPE OF REPORT & PERIOD COVERED: Interim rept.
	6. PERFORMING ORG. REPORT NUMBER: TR-0080(5950-01)-1
7. AUTHOR(s): Ernest G. Wolff	8. CONTRACT OR GRANT NUMBER(s): F04701-79-C-0080
9. PERFORMING ORGANIZATION NAME AND ADDRESS: The Aerospace Corp. El Segundo, Calif. 90245	10. PROGRAM ELEMENT, PROJECT, TASK AREA & WORK UNIT NUMBERS: 12 93
11. CONTROLLING OFFICE NAME AND ADDRESS: Space Division, Air Force Systems Command, Los Angeles Air Force Station, Los Angeles, Calif. 90009	12. REPORT DATE: 1 Sep [redacted]980
	13. NUMBER OF PAGES: 34
14. MONITORING AGENCY NAME & ADDRESS (if different from Controlling Office)	15. SECURITY CLASS. (of this report): Unclassified
	15a. DECLASSIFICATION/DOWNGRADING SCHEDULE

16. DISTRIBUTION STATEMENT (of this Report)

Approved for public release; distribution unlimited

17. DISTRIBUTION STATEMENT (of the abstract entered in Block 20, if different from Report)

18. SUPPLEMENTARY NOTES

19. KEY WORDS (Continue on reverse side if necessary and identify by block number)

Acoustic Emission
Composite Materials
Dimensional Stability
Graphite-Epoxy
Mechanical Properties
Microcracking
Micromechanics

20. ABSTRACT (Continue on reverse side if necessary and identify by block number)

Microcracking in composite materials is commonly caused by ply stiffness variations in crossply layup during application of applied stress, and by differential thermal expansion coefficients of the fiber and the matrix during thermal excursions. It is responsible for changes in macro- and micromechanical properties, permeability to gases, and dimensional instability. Theories, experimental techniques, and effects of microcracking are reviewed. The coefficient of cracking expansion is defined, and procedures for reducing deleterious effects of microcracking on composite structures are presented.

DD FORM 1473 (FACSIMILE)

403 644

UNCLASSIFIED

SECURITY CLASSIFICATION OF THIS PAGE (When Data Entered)

CONTENTS

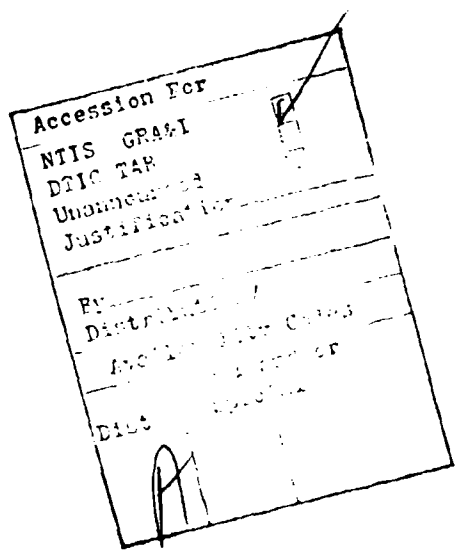

FIGURES

TABLES

I. INTRODUCTION

Microcracking is the self-descriptive, common response of most materials to internal stresses. In metals and alloys it may be caused by coalescence of dislocations or interaction of slip bands during plastic deformation. Commonly it occurs in all materials when there are dimensional mismatches between discrete phases or constituents, as in precipitation hardening of alloys or in thermal excursions of fiber reinforced composites used on spacecraft. The microcrack represents a local geometrical change that can be multiplied into unacceptable dimensional, or other property, changes of a component or structure.

Microcracking alters mechanical properties, permeability to gases or moisture, and dimensional stability. Considerable attention has been paid to its effects on fatigue and strength properties of composites, such as tensile, interlaminar shear, flexure, and stiffness properties (e.g., for aircraft composite applications). However, there has been relatively little work on dimensional stability. Studies have included microcracking effects on the coefficient of thermal expansion (CTE), coefficient of moisture expansion (CME), microyield strength, and dimensional changes after thermal cycling.

The basic elements of this report were presented at an Aerospace Symposium on Non-Destructive Testing on February 21, 1979.[1] This report also provides an introduction to Aerospace studies on acousto-optical methods of measuring microcracking characteristics.[2]

II. THEORIES OF MICROCRACKING

There are diverse causes, mechanisms, and composite materials factors involved in the general process of microcracking. The causes of microcracking in composites are as follows: cooling from cure/fabrication temperature; thermal excursions; applied stresses; moisture induced stress changes; and radiation induced structural changes. The mechanisms of microcracking are fiber breaks, splits; matrix or interfiber cracks; delamination; debonding or fiber pullout; and growth of flaws or voids. The composite materials factors involved in microcracking are ply layup (90° plies susceptible); flaws, voids, surface cracks; resin, interlayers (T_g, T_c, E_m, V_m); moisture level; loading or stress level; temperature, time, history - viscoelastic effects; end, edge effects; and fiber parameters (twist of tow, ε_u, V_f). The first mode of cracking to initiate depends on the stress field and various composite characteristics, such as E_f, V_f, stacking sequence, or ply thickness. Determination of the initial mechanism of microcracking is the subject of References 3 through 7. The most recent reference, L. Rotem and Altus,[6] bases its criteria on the critical elastic energy release or absorption rate G_c and the relationship of G_c to the stress intensity factor K_c. For example, when a crack propagates parallel to an unfractured fiber

$$G_c = K_c^2 \left(\frac{S_{11}S_{22}}{2}\right)^{1/2} \left[\left(\frac{S_{11}}{S_{22}}\right)^{1/2} + \left(\frac{2S_{12} + S_{66}}{2S_{22}}\right)\right]^{1/2} \qquad (1)$$

where S_{ij} represents the elastic compliances. By contrast, the matrix failure perpendicular to the fibers yields an energy-release rate similar to that for isotropic materials.

$$G_c = \frac{K_c^2}{E_T} \qquad (2)$$

The failure point for cracks parallel to the fibers is also expressed as[3]

$$\left(\frac{\sigma_A E_m}{E_A \sigma_T}\right)^2 + \left(\frac{\sigma_T}{\sigma_s}\right)^2 + \left(\frac{\tau}{\tau_s}\right)^2 = 1 \qquad (3)$$

Further studies of crack propagation composites, based on stored elastic strain energy, are represented by References 8 through 13. For example, Beamont and Harris[10] found that, for crack propagation parallel to fibers, the work of fracture γ_F and stored elastic strain energy per unit of fracture surface during initiation of microcracking γ_I are similar and not unlike the fracture surface energy of the resin alone. The corresponding stress intensification at the tip of the crack is

$$K_{Ic} = 2E\,\gamma_{Ic} \qquad (4)$$

and for an unreinforced resin (828/DDM),

$$K_{Ic} = 1.20 \text{ MN m}^{-3/2}$$

$$\gamma_{Ic} = 345 \text{ Jm}^{-2}$$

$$\gamma_F = 330 \text{ Jm}^{-2}$$

where 1 J = 1 N - m. Moisture and voids tend to lower the above values by a few percent. Griffiths and Holloway[11] suggest $\gamma_{Ic} = 10^3$-10^5 ergs/cm^2 ~ 1-100 Jm^{-2} but filled resins have values up to 500 Jm^{-2}. Here, γ_{Ic} does not vary appreciably with crack area for an unreinforced resin.[12]

Sih and co-workers[7,9] combine laminate theories and strain energy density considerations. A matrix crack propagation model establishes a strain energy density factor

$$\Sigma = S_{11}k_1^2 + 2S_{12}k_1k_2 + S_{22}k_2^2 \qquad (5)$$

where k represents stress intensity factors, in turn, dependent on geometry and elastic and loading properties. The condition $\partial\Sigma/\partial\theta = 0$ determines the direction of crack propagation θ_o. The critical strain energy density Σ_c at θ_o determines the onset of unstable crack propagation. The effects of ply orientation on failure mode are also discussed in Reference 5.

Shear lag analyses[14,15] are of particular interest to dimensional considerations because they deal with strain release due to crack formation. It must be noted that matrix cracking can occur at composite strain levels considerably below resin failure strains. Cross-ply laminates are particularly susceptible, with microdamage commonly originating at the "knee" of the stress-strain curve.

The initiation of matrix cracking by low-temperature thermal excursions has been investigated.[1,2,16-18] A simplified expression for the axial stress in the matrix of a unidirectional composite was given by Sambell[16]

$$\sigma_a = (\alpha_m - \alpha_f)\Delta T \left[\frac{E_f V_f}{V_f \left(\frac{E_f}{E_m} - 1 \right) + 1} \right] \qquad (6)$$

where ΔT refers to the excursion from the stress-free temperature (typically 270°F for a 350°F cure). Point-stress analysis can be used[2] to predict the onset temperatures for microcracking, which occurs when the transverse laminate strength is exceeded in the multi-ply composite. Some experimental results are summarized in Table 1.[2,17]

Expected degradation of G_{12} and E_{22} of a composite after moderate matrix microcracking was found to have negligible effects on the expansion characteristics.[2] Delamination is difficult to model analytically.[3,6,7]

Table 1. Onset Temperatures for (Thermal) Microcracking

Composite System	Layup	T_c (°F)	T_{onset} (°F)	Reference
GY 70/934	0/±60/0	350	-22	Aerospace
GY 70/934	±30/∓30	350	-130	Aerospace
HMS/3501-6	90/0/±45	350	-50	Aerospace
T 300/934	Multi-ply Fabric	350	-100 to -320	Kirlin/Pynchon
GY 70/X30	$(0/45/90/135)_s$	250	-170	General Dynamics/Convair Division
GY 70/934	0°	350	-16	Aerospace - predicted
GY 70/X904	pseudo/isotropic	375	7 R.T.	General Dynamics/Convair Division

Microcracking is also described in terms of the Kaiser and Felicity effects.[19] "Elastic bodies tend to exhibit no microcracking when reloaded to the same level," is a statement of the Kaiser effect. However, epoxies do not exactly follow this effect. The Kaiser effect may be useful in determining the previous maximum stress in a body, at least if the stress is predominantly uniaxial and tensile.[20] Matrix crazing is dependent on previous load history, but does not follow the Kaiser effect at either low or high loads or stress states. Immediate unloading (or heating after cooling below an onset temperature) allows some stress redistribution, and cracking may continue to lower levels due to the viscoelastic matrix (Felicity effect).

The composite materials factors previously listed influence the stress states, K_{IC}, and γ_{Ic} and modulus near ends or edges. Viscoelastic effects, for example, change internal stress states.

III. EXPERIMENTAL TECHNIQUES

Methods for the experimental investigation of microcracking phenomena are few and include stress strain testing[14,15] coupled with microstructural examination.[14,18,21,22] Relatively nondestructive techniques include ultrasonics and radiography[23,24] and acoustic emission (AE).[3,8,20,23,25-27] The latter technique is the most useful as it detects in real time, sound waves generated by individual cracking events. A variety of signal processing techniques [total counts, root-mean-square (rms), frequency analysis, amplitude distribution, energy/real time] and transducers (piezoelectric, capacitance, strain gauge, optical) permit considerable knowledge to be gained of the microcracking process.

The AE technique was originally used to study crack growth in materials and to detect fiber breaks in composites. More recently, emphasis has been placed on the determination of the predominant microcracking mechanism. This has involved three principle experimental approaches: count rate, frequency analysis, and amplitude distribution analysis. The first approach is the easiest to use, and is particularly effective in designating temperatures and stress levels for the onset of microcracking and demonstrations of the Kaiser effect,[3,12,26,28-30] the effects of strain rates,[31] and the influences of fiber, matrices, and layup. The identification of predominant mechanisms for microcracking generally requires more than integration of burst amplitudes above an arbitrary signal level in a transducer. One technique has been the monitoring of the rms signal level in real time. Thus, low level energy events such as interfiber fracture can generally be distinguished from high energy fiber breaks.[28]

Another approach, frequency analysis,[3,28,32-34] involves a study of pulse shapes by Fourier methods. In this case, signals are affected by attenuation and dispersion in the composite and by variability between frequency spectra within emission events of the same type. Normalized spectral energy distributions,[33] deconvolution techniques to isolate AE sources,[35] and computerized pattern recognition technique[36] are some newer methods for the identification of AE mechanisms.

The AE transducers have severe limitations: they load the surface and disturb the transients to be measured; their mechanical resonances modify recorded signals; their frequency response is limited to the 100 KHz to 2 MHz range (and is not usually linear even within that range); and they have unpredictable response characteristics and show increased noise levels when operated in vacuo to cryogenic temperatures. Optical sensing of AE phenomena was first reported by Palmer and Green,[37] who point out the numerous advantages of this technique over the use of transducers, including the capacity for measurement of the absolute amplitude and phase of acoustic disturbances. Optical laser beam probes coupled with fast-digital-signal processing systems are able to capture the initial transient of the true AE signal source, whereas "ringing" of conventional piezoelectric transducers (PZTs) dominate the recorded signals.[15,38] The use of reflected, rather than transmitted, beams for analysis of AE due to matrix cracking has recently been explored at Aerospace.[2] Advantages of this technique over the use of conventional transducers are: flat frequency response; low-frequency for increased sensitivity; low-frequency signal for less attenuation; elimination of AE transducer problems, e.g., low temperature, allows pulse shape (frequency) analysis; ability to study effect of AE on natural vibrations. A comparison of the technique that demonstrates the sensitivity of the optics was performed by obtaining coincident counts from a stereo tape playback. It was found that for eight times greater than about 1 ms, the optics recorded over 98% of the cracks that were detected by the PZT, whereas the PZT detected only 6% of the cracks detected by the optics. The opto-acoustic technique has on-board or ground-based applications and can be used for nondestructive testing of spacecraft in flight and for pressurization of rocket motor cases.

Capacitance[3] and strain-gauge transducers[34] offer other alternatives to PZTs. The former is another contactless method, whereas the latter is a low cost means for possible long-term monitoring of defect generation.

Finally, the experimental approach of amplitude distribution analysis[3,6,25,32,39] has been used for the discrimination of microcracking mechanisms by recognition that the amount of energy varies with each failure mode and that the AE pulse is proportional to the strain energy released. The

predominant failure mode can be determined by measurement of the exponent in the relation $I = I_o D^{-n}$, where I is the count rate, and D the discrimination level. Here, n is generally 1.1 to 1.6 for interfiber failure and 0.6 to 0.8 for fiber fracture in graphite-epoxy (Fig. 1). The measuring of counts, or the exceeding of a certain energy level per microcracking event, is another means for discrimination of cracking mechanisms.[19,39]

The effect of ply layup on AE has been reviewed by Williams and Lee.[20] When fiber fracture is known to occur, fibers oriented at 30° to the loading axis generate more AE counts than those oriented at 0 and 90°. Multiple fractures of each filament are then likely to occur. The amplitude of the AE count rate decreases with 0, 90, and 15, 30 and 45° fiber fractures. Fiber fracture in general is more energetic than other failure modes.

A convenient method for the prediction of the magnitude of laminate residual stresses is by a behavior analysis of nonsymmetric "flat" laminates.[40,41] Tubes have the advantage of reduced edge effects. They can be anisotropic and still remain round, but they may twist. The twisting of tubes can be measured then with auto-collimators.[42]

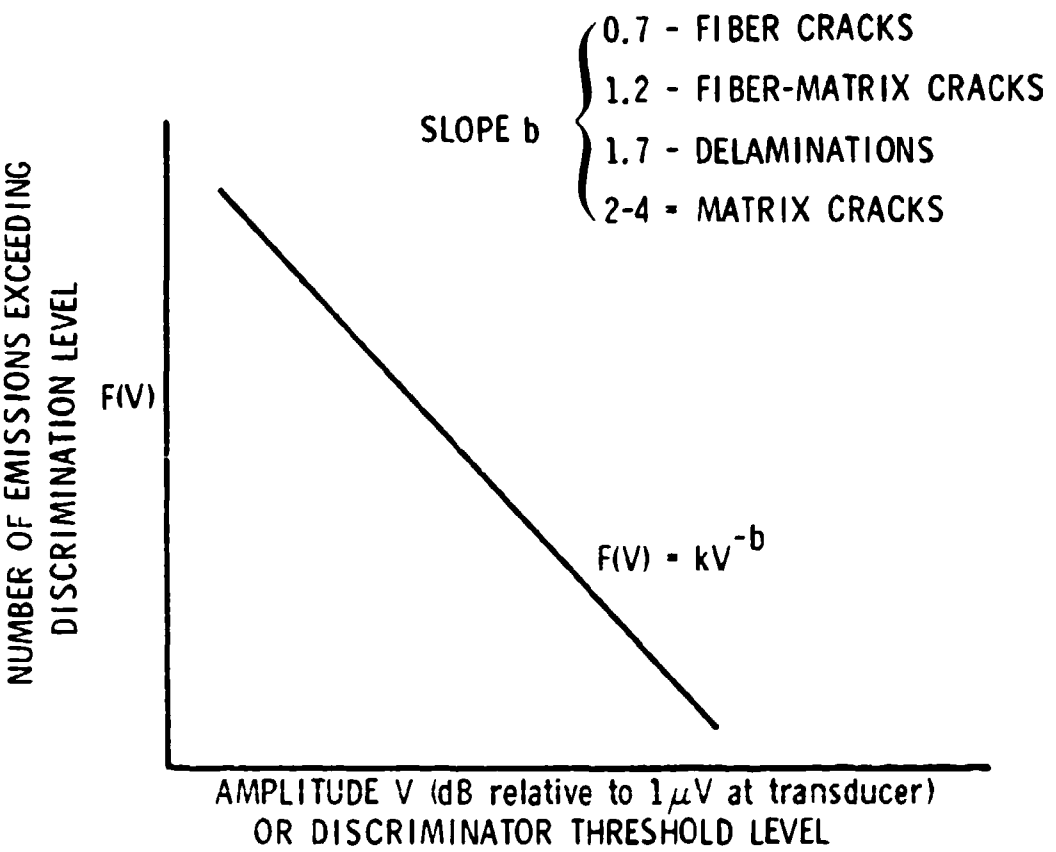

Fig. 1. Identification of Degradation Process by Acoustic Emission Amplitude Distribution Analysis for GFRP

IV. EFFECTS OF MICROCRACKING

Examples of some effects of microcracking on mechanical dimensional stability and related properties are described in the following subsections.

A. TENSILE AND STIFFNESS PROPERTIES

Failure strains of greater than 20% may be needed for the resins used in cross-ply laminates to develop optimum strength.[43] Indeed, mechanical properties change less when the resin elongation at fracture increases.[14] Stiffness changes are generally greater than 20%.[19,44] Flatwise tensile strength of laminates, especially thick ones, is usually reduced when microcracking has occurred.[21] Thick samples are more prone to thermal shock on rapid cooling and therefore to more microcracking. Compressive strength tends to decrease in the fiber direction due to interfacial bond limitations.

B. INTERLAMINAR SHEAR AND FLEXURE

Interlaminar shear stiffness decreases unless thermal cycling is carried out to high temperature (near the cure temperature), at which point the shear strength may actually increase. Flexure properties also tend to be temperature dependent. Post-curing helps flexure properties, with or without microcracking.

C. FATIGUE AND DAMPING

A high matrix modulus helps to maximize fatigue life, since matrix damage is a principal failure mechanism here, even with metal matrix composites. Microcracking significantly enhances the ability of a composite to dissipate energy, e.g., through frictional losses between opposing faces of the crack.[19] Damping is enhanced if fiber matrix interface cracks occur rather than cracks only in the matrix. The fiber-matrix bond strength will be a major factor in the determination of damping changes due to microcracking. Fatigue life of composites may also be frequency dependent, as found for boron-epoxy systems.[43] Low cycle fatigue does not significantly affect other structural design parameters, even if moderate microcracking occurs.[45]

D. MOISTURE INTERACTIONS

Interfiber cracks may appear when essentially dry graphite-epoxy is exposed to a humid environment, especially if an unsymmetric laminate is involved.[46] In this case, the cracking rate is affected by the cooldown rate from the cure temperature, by postcuring conditions, and by temperature distributions. The following is a summary of moisture effects on microcracking: curing stresses reduce the applied stresses needed for initial matrix cracking in (transverse) plies by about 50%; moisture may eliminate the above effect and even increase required stress; moisture gradients may cause unequal swelling leading to microcracks; and moisture may also degrade the fiber-matrix interface bond.

E. COEFFICIENT OF THERMAL EXPANSION

Decreases in apparent CTE occur with thermal cycling. The obvious explanation is that with reduced contact between fiber and matrix, the negative CTE fiber tends to dominate. Alternatively, with delamination, the angle plies may reduce their contribution to the CTE in a given direction. However, theoretically, the CTE can go either positive or negative, depending on the fiber, resin, residual stress state, ply layup, and type of microcracking. Since there is often an expansion associated with microcracking, a positive CCE, this is easily confused with changes in CTE. The presence of a core material increases the number of cycles necessary to reach a CTE asymptote from 5 to 10 to several thousand cycles (Fig. 2).[21,47,48] Hence, there is a need to specify the temperature range as well as the hygro-thermomechanical history of a given CTE measurement.

F. THERMAL CYCLING

High interlaminar stresses, caused by thermal cycling, tend to occur close to the edges between cracked and uncracked laminae; the interiors of these may be relatively stress free.[26] Voids may also play a role in initiating microcracks.[21] Sandwich cores increase stresses in the laminates near the bond line, and microcracking is enhanced in adjacent plies. The temperature at which tensile microfracture occurs in the epoxy depends mainly on the fiber and resin system and on the ply layup and usually falls between room

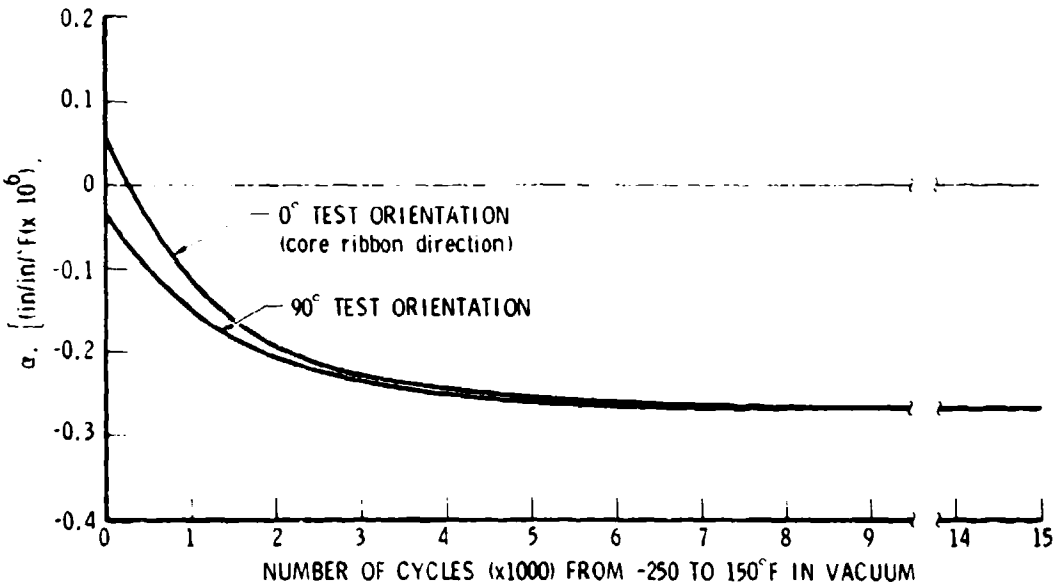

Fig. 2. Effect of Thermal Cycling in Vacuum on Thermal Expansion of GY 70/934 Sandwich (TRW data)

temperature and -200°F. The stress relaxation associated with thermal cycling leads to dimensional instability. This cannot, in principle, be prevented by design of the composite for a near zero CTE. Net dimensional changes after cycling to low-temperature excursions are usually caused by microcracking and are on the order of 10 to 50 × 10^{-6} in/in[49] (Figs. 3 and 4).

G. MICROCREEP AND MICROYIELD

The matrix is important in creep phenomena, and nonlinear viscoelastic effects may be expected. Some unusual effects, with possibly competing deformation mechanisms, tend to result from the ±45° orientation. However, there are virtually no data on direct microcracking effects.

The microyield strain (MYS) is dramatically affected by microcracking, with over 90% reductions in strength values after thermal cycling to liquid nitrogen temperatures. Stress-residual strain data after short-term loading tests are shown in Fig. 5. The difference between the curves is due primarily to microcracking.[50]

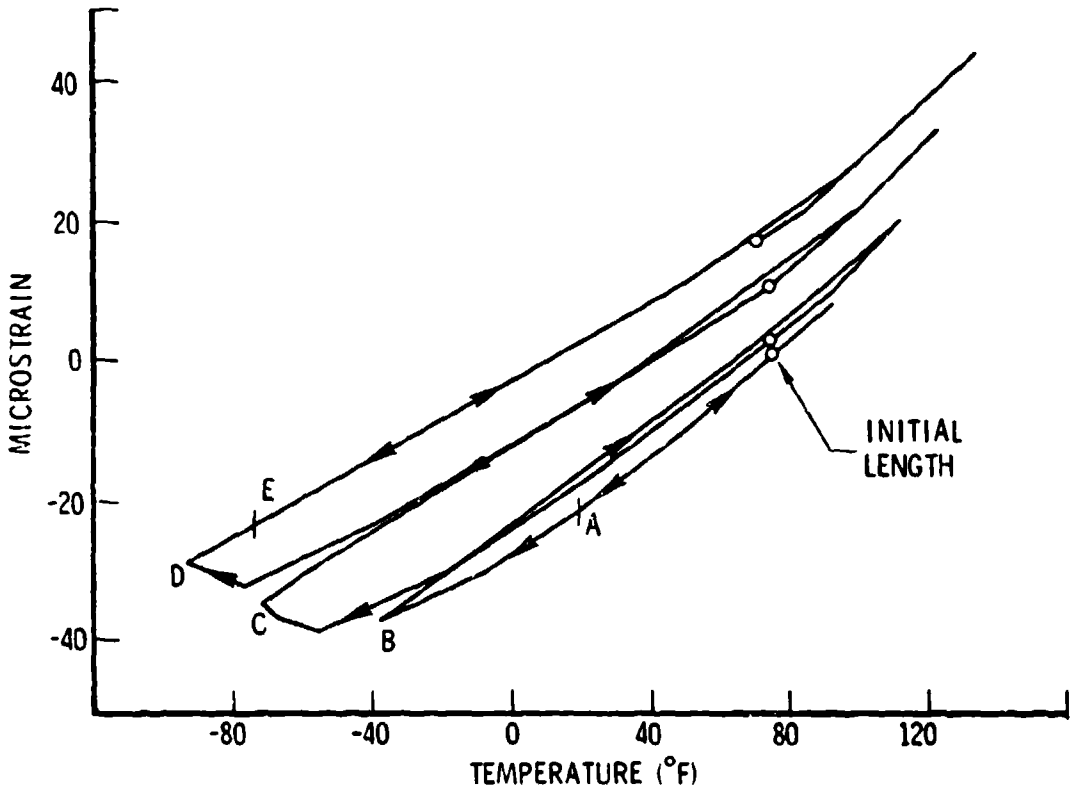

Fig. 3. Thermal Cycling of a Graphite-Epoxy Tube

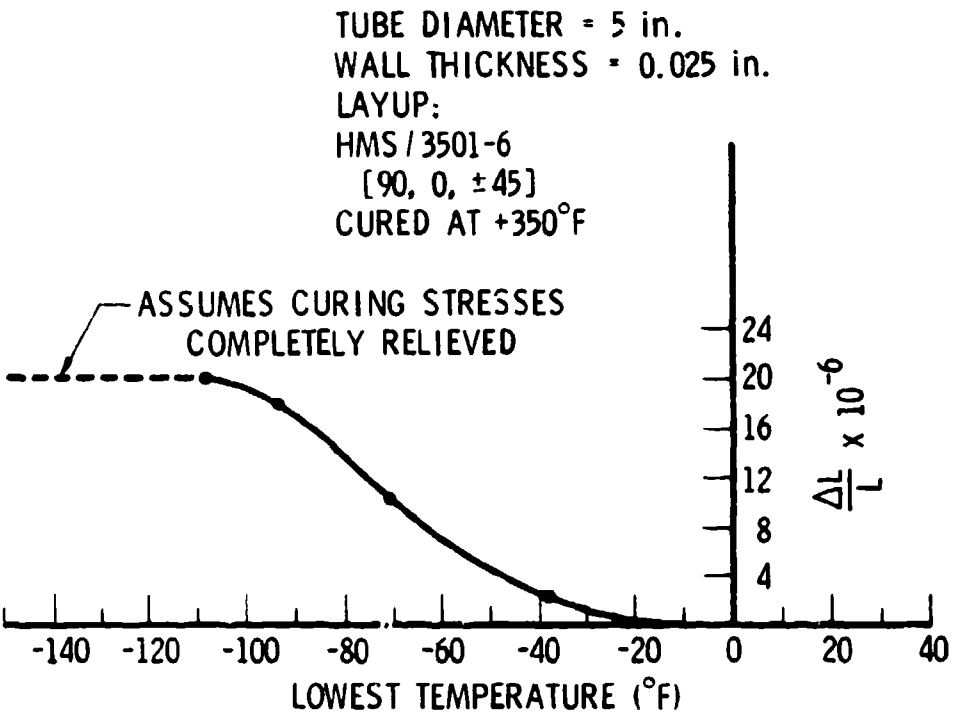

Fig. 4. Supporting Test Data for Rib Microcracking Strain[36]

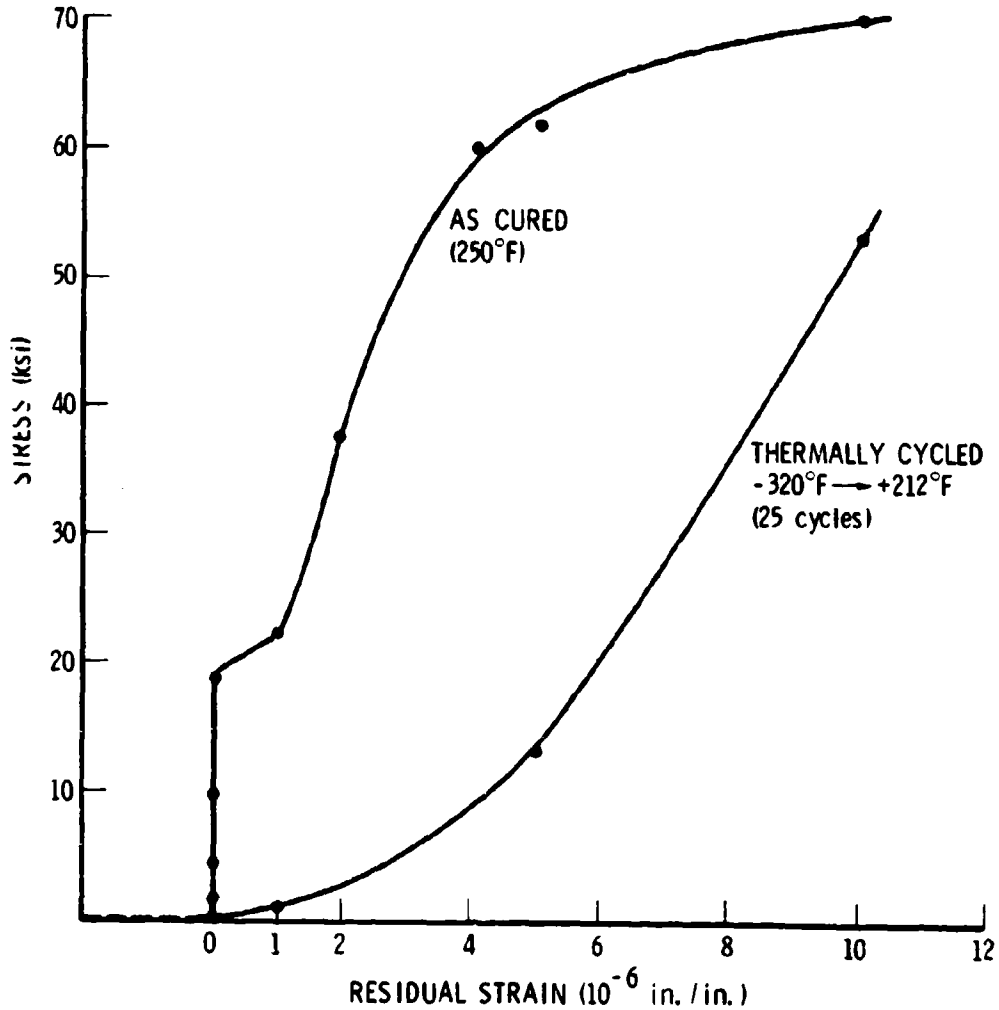

Fig. 5. Microyield Data for HMS/339 Oriented Laminate[50]

V. COEFFICIENT OF CRACKING EXPANSION

The macroscopic dimensional change resulting from internal crack generation is a relatively new topic in materials science and requires highly sophisticated instrumentation. The opto-acoustic technique discussed previously is ideally suited for such studies and enables comparisons of acoustic activity to be made with dimensional changes (Fig. 6). In this instance, the expansion measured during AE activity is separated into a cracking expansion and a thermal expansion. The latter is apparent from subsequent thermal excursions (pseudo-Kaiser effect) or extrapolated thermal $\Delta L/Ls$ from the first cooling cycle. An audio recording of the rms optical output to 20 KHz, with voltage output proportional to crack induced displacements to approximately 1000 Å, may be fed into a spectrum analyzer with a memory scope. After an allowance is made for internal echoes, the crack events may be counted per unit time and compared to the cooling rate (Fig. 7). The straight-line relationship combined with the zero intercept suggest all cracks were counted (on initial cooling cycles), and the slope dN/dT equals 46 cracks/°F for this sample (0/±60/0, GY 70/934 tube).[2] The measured $\gamma_o = \partial\varepsilon/\partial T = -0.123 \times 10^{-6}$ in/in/°F. One can calculate $\partial\sigma/\sigma T$ as 13 psi/°F from laminate theory. If these quantities are combined, the values become

$$\partial\sigma/\partial N = (\partial T/\partial N)(\partial\sigma/\partial T) = 0.28 \text{ psi/crack}$$

$$\partial\varepsilon/\partial N = (\partial T/\gamma N)(\partial\varepsilon/\partial T) = 2.7 \times 10^{-9} \text{ in/in/crack}$$

$$(\partial\varepsilon/\partial N)(\ell o) = 24 \text{ Å/crack}$$

where l_o is the sample length in the displacement direction. Additional studies are needed to establish γ_{11} and γ_{22} as laminate design parameters. Comparison with shear lag theory (see Section II) is also in order to predict

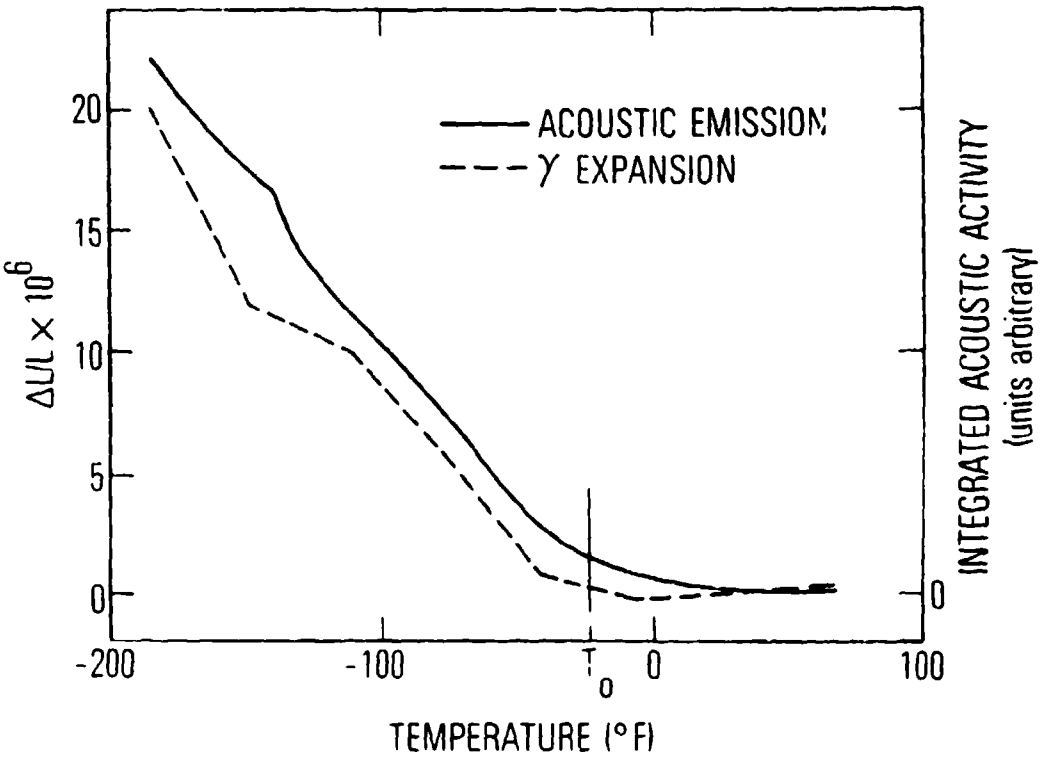

Fig. 6. Comparison of Acoustic Activity with Dimensional Changes

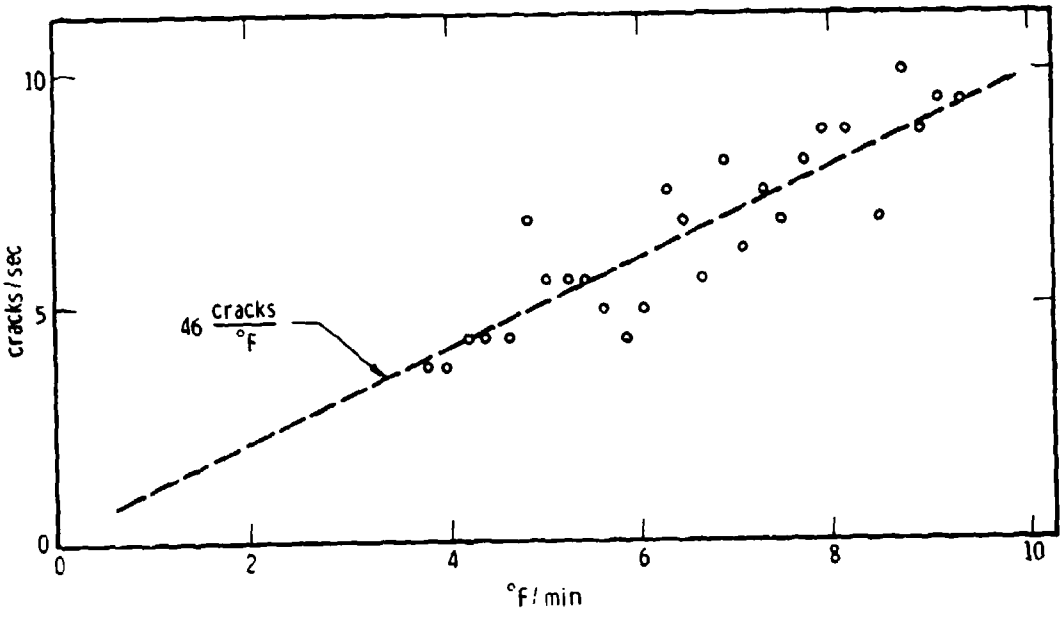

Fig. 7. Detected Crack Rate (Acoustic Events) versus Temperature Rate 0/±60/0 Tube

crack displacements with optimum microcracking models. Further studies would have to consider viscoelastic, edge, and moisture effects, and possibly corrections for attenuation within the composite. There may also be possibilities to measure the energy per crack and comparisons to the energy based theories in Section II.

VI. REDUCTION OF MICROCRACKING

Methods for minimizing microcracking and its effects in composite materials are summarized below:

- Postcure annealing (increase E_m)
- Keep H_2O in matrix (reduce effective curing σ)
- Use of weaves/fabrics (crack arrests)
- Low T_c (increase matrix failure ϵ)
- Transverse stiffeners (e.g., glass fabrics, increase "E_m")
- Minimize yarn/tow twist (reduce f-f contacts)
- Particulate additives (lower CTE_m)
- Uniform ply distribution (localize interfiber cracks)
- Cycle below T_{min} of use (preconditioning)

Composites with high-modulus fibers and low CTE values are prone to microcracking. Large numbers of plies in one direction should be minimized if they are sandwiched between angle plies. The resin can be modified to increase its yielding and cold-drawing capabilities under stress. Both a high-matrix modulus and a high elongation to failure are desirable. (The hardening from cold flow tends to relieve the stress concentrations between the fibers.)[10,51] It is desirable to minimize resin shrinkage after gelation, as well as its thermal expansion characteristics and cure temperature. The problem with a low-cure temperature, however, is that this also leads to a low glass transition temperature, and moisture cannot be safely removed through high-temperature treatment. The use of balanced and symmetric layups, and the interspersion of soft or plastic plies also help to prevent interlaminar cracking.

A summary of major effects of microcracking with related references is given in Table 2.

Table 2. Effects of Microcracking

Property	System	Effect: Example	References	Other References
Tensile Strength	GY 70/934	Reduction on cooling to -320°F	21	
	HMS/3501	0° tensile, 97 to 85 Ksi	50	18,22,43,52
		90° tensile may increase	53	
Stiffness	glass/resin	0/90/90/0 E_2 ~ 70% of E_1	18	53
	HMS/3501	E_{90} decrease on cycling to low temperature	50	
		E_o may increase	53	
Compressive Strength		Decrease in 0° direction	53	
Interlaminar Shear Strength (ISS)		Increased by cycling to high temperature	53	14,54
		ISS decrease	26	
Flexure Strength		Increase/decrease on thermal cycling	53	21,22
Fatigue Strength		Reduces cycles to failure and possibly mode of failure	39	34,45
		Weaves and/or high matrix modules helpful	55	
Damping	GY 70/339	90/±45/90 loss factor increases	56	57
		2 to 20 x increase	58	58
Permeability to H_2O/gases		GY 70/339 at 180°F, double absorption rate	40	18,26,59,60,61
		Reduced lowering of T_g as % moisture increases	62	
Thermal Expansion	HM/934	α_o from 0.21 to 0.16 ppm/°F	17	21,49
	T300 fabric	0.88 to 0.58 ppm/°F	17	
	HMS/3501 oriented	-0.13 to -0.26 ppm/°F	50	
Thermal Cycling	HMS/3501	Net ΔL/L of ~?0 ppm	2, 49	17,26,50,51,53,63
Microcreep	GY 70/X904	Weak areas show increased creep	35	
Microyield Strength	HMS/934 (unidirectional)	40 to 4.5 Ksi	50	14,48
	HMS/389	23.3 to 1 Ksi	50	

REFERENCES

1. E. G. Wolff, "Microcracking in Graphite/Epoxy Composites," Paper presented Aerospace NDT Symposium, 21 February 1979.

2. S. A. Eselun, H. D. Neubert, and E. G. Wolff, "Microcracking Effects on Dimensional Stability," The Enigma of the Eighties: Environment, Economics, Energy, Vol. 24, SAMPE, Azusa, Calif. (1979), pp. 1299-1309.

3. A. Rotem, "The Discrimination of Micro-Fracture Mode of Fibrous Composite Material by Acoustic Emission Technique," Fibre Sci. Tech. 10 (2), 101-121 (1977).

4. A. Rotem and Z. Hash, "Failure Modes of Angle Ply Laminates," J. Comp. Mat. 9, 191-206 (1975).

5. V. G. Grinius, "Micromechanics-Failure Mechanism Studies," Paper presented 22nd Annual Meeting of SPE, Washington, D.C. (1967).

6. A. Rotem and E. Altus, "Fracture Modes and Acoustic Emission of Composite Materials," J. Test. Eval. 7 (1), 33-40 (January 1979).

7. G. C. Sih and E. P. Chen, Fracture Analysis of Unidirectional Composites, NADC-TR-73-1, Lehigh University, Bethlehem, Penn. (1973).

8. W. E. Swindlehurst and C. Engel, "A Model for Acoustic Emission Generation in Composite Material," Fibre Sci. Tech. 11 (6), 463-479 (1978).

9. G. C. Sih et al., "Material Characterization on the Fracture of Filament-Reinforced Composites," J. Comp. Mat. 9, 167-186 (April 1975).

10. P. W. Beaumont and B. Harris, "The Energy of Crack Propagation in Carbon Fibre-Reinforced Resin Systems," J. Mat. Sci. 7, 1265-1279 (1972).

11. R. Griffiths and D. G. Holloway, "The Fracture Energy of Some Epoxy Resin Materials," J. Mat. Sci. 5, 302-307 (1970).

12. J. Fitz-Randolph et al., "The Fracture Energy and Acoustic Emission of a Boron-Epoxy Composite," J. Mat. Sci. 7, 289-294 (1972).

13. J. N. Kirk, M. Munro, and P. W. Beaumont, "The Fracture Energy of Hybrid Carbon and Glass Fibre Components," J. Mat. Sci. 13, 2197-2204 (1978).

14. K. W. Garrett and J. E. Bailey, "Multiple Transverse Fracture in 90° Cross-Ply Laminates of a Glass Fibre Reinforced Polyester," J. Mat. Sci. 12, 157 (1977).

15. A. Parvizi and J. E. Bailey, "On Multiple Transverse Cracking in Glass Fibre Epoxy Cross Ply Laminates," J. Mat. Sci. 13, 2131-2136 (1978).

16. R. A. Sambell et al., "Carbon Fibre Composites with Ceramic and Glass Matrices," J. Mat. Sci. 7, 676-681 (1972).

17. R. L. Kirlin and G. E. Pynchon, "Dimensional Stability Investigation - Graphite/Epoxy Truss Structure," The Enigma of the Eighties: Environment, Economics, Energy, Vol. 24, SAMPE, Azusa, Calif. (1979), pp. 1356-1371.

18 G. T. Stevens and A. W. Lupton, "Transverse Cracking in Cross-Plied Composites," J. Mat. Sci. 11, 568-570 (1976).

19. T. J. Fowler, "Acoustic Emission Testing of Fiber Reinforced Plastics," Paper presented ASCE Fall Convention and Exhibit, 17-21 October 1977.

20. J. H. Williams and S. S. Lee, "Acoustic Emission Monitoring of Fiber Composite Materials and Structures," J. Comp. Mat. 12, 348-370 (October 1978).

21. L. D. Berman, "Reliability of Composite Zero-Expansion Structures for Use in Orbital Environment," Composite Reliability, ASTM-STP-580, ASTM, Philadelphia, Penn. (1975), pp. 288-297.

22. R. A. Mayor, "Advanced Composites for High Temperature Applications," Materials and Processes - In Service Performance, Vol. 9, SAMPE, Azusa, Calif. (1977), pp. 478-490.

23. C. D. Bailey, S. M. Freeman, and J. M. Hamilton, "Detection and Evaluation of Impact Damage in Graphite/Epoxy Composites," Materials and Processes - In Service Performance, Vol. 9, SAMPE, Azusa, Calif. (1977), pp. 491-503.

24. J. L. Camahort et al., "Process Control NDE Procedures for Advanced Composite Structure," The Enigma of the Eighties: Environment, Economics, Energy, Vol. 24, SAMPE, Azusa, Calif. (1979), pp. 377-389.

25. J. Becht, H. J. Schwalbe, and J. Eisenblaetter, "Acoustic Emission as an Aid for Investigating the Deformation and Fracture of Composite Materials," Composites, 245-248 (October 1976).

26. A. Molcho and O. Ishai, "Thermal Cracking of C.F.R.P. Laminates," Materials Synergisms, Vol. 10, SAMPE, Azusa, Calif. (1978), pp. 255-262.

27. D. O. Harris, A. S. Tetelman, and F. A. Darwish, Detection of Fiber Cracking in Acoustic Emission, TR-DRC-71-1, Dunegan Corp., Livermore, Calif. (February 1971).

28. F. J. Guild et al., "The Application of Acoustic Emission to Fibre-Reinforced Composite Materials," Composites, 173-179 (July 1976).

29. M. A. Hamsted and T. T. Chiao, "Acoustic Emission from Stress Rupture and Fatigue of an Organic Fiber Composite," Composite Reliability, ASTM-STP-580, ASTM, Philadelphia, Penn.(1975) pp. 191-201.

30. C. B. Scruby and H. N. Wadley, "A Calibrated Capacitance Transducer for the Detection of Acoustic Emission," J. Appl. Phys. 2, 1487-1494 (1978).

31. A. Rotem, "Effect of Strain Rate on Acoustic Emission from Fibre Composites," Composites, 33-36 (January 1978).

32. L. J. Graham, Characterization of Acoustic Emission Signals and Application to Composite Structures Monitoring, AFML-TR-77-44, AFML, Dayton, Ohio (September 1977) pp. 40-45.

33. J. H. Williams and D. M. Egan, "Acoustic Emission Spectral Analysis of Fiber Composite Failure Mechanisms," Mat. Eval. 43 (January 1979).

34. R. G. White and H. Tretout, "Acoustic Emission Detection Using a Piezoelectric Strain Gauge for Failure Mechanism Identification in CFRP," Composites, 101-109 (April 1979).

35. N. P. Freund, Measurement of Thermal and Mechanical Properties of Graphite/Epoxy Components for Precision Applications, ASTM-STP-580, ASTM, Philadelphia, Penn. (1975) pp. 133-145.

36. M. R. Sullivan and B. E. McIntosh, "Space Deployable Antenna Applications of Metal Matrix Composites," Paper presented Aerospace Corp., El Segundo, Calif., 10 July 1979.

37. C. Harvey Palmer and R. E. Green, "Optical Detection of Acoustic Emission Waves," Appl. Opt. 16 (9), 2333-2334 (September 1977).

38. B. B. Djordjevic and R. E. Green, "High Speed Digital Capture of Acoustic Emission and Ultrasonic Transients as Detected with Optical Laser Beam Probes, Paper presented 79th Ultrasonics International Conference, Graz, Austria, May 1979.

39. J. T. Ryder and J. R. Wadin, Acoustic Emission Monitoring of a Quasi-Isotropic Graphite/Epoxy Laminate Under Fatigue Loading, Dunegan/Endevco, San Juan Capistrano, Calif. (1979).

40. R. E. Mauri, F. W. Crossman, and W. J. Warren, "Assessment of Moisture Altered Dimensional Stability of Structural Composites," Selective Application of Materials for Products and Energy, Vol. 23, SAMPE, Azusa, Calif. (1978) pp. 1202-1217.

41. F. W. Crossman and D. L. Flaggs, "Dimensional Stability of Composite Laminates during Environmental Exposure," 15th National SAMPE Technical Conference, Vol. 15, SAMPE, Azusa, Calif., pp. 15-20.

42. E. G. Wolff and S. A. Eselun, "Thermal Expansion of a Fused Quartz Tube in a Dimensional Stability Test Facility," Rev. Sci. Instrum. 50 (4), 502-506 (April 1979).

43. J. A. Kies, Report 5752, U.S. Naval Research Laboratory, Washington, D.C. (1962).

44. B. W. Rosen, "Tensile Failure of Fibrous Composites," AIAA J 2 (11), 1985 (November 1964).

45. A. Parvizi and J. E. Bailey, "On Multiple Transverse Cracking in Glass Fibre Epoxy Cross Ply Laminates," J. Mat. Sci. 13, 2131-2136 (1978).

46. H. T. Hahn and R. Y. Kim, Swelling of Composite Laminates, AFML-TR-77-199, AFML, Dayton, Ohio (September 1977).

47. N. L. Hancox and D. C. Minty, "Materials Qualification and Property Measurements of Carbon Fibre Reinforced Composites for Space Use," J. Brit. Interplanetary Society 30, 391-399 (1977).

48. F. L. Mathews and H. C. Kim, "Tensile Microstrain and Cyclic Behavior in CFRP," Properties of Fibre Composites-Conference Proceedings, IPC Sci. Tech. Press Ltd., Guilford, United Kingdom (1971), pp. 57-59.

49. E. G. Wolff, "Measurement Techniques for Low Expansion Materials," Materials and Processes - In Service Performance, Vol. 9, SAMPE, Azusa, Calif. (1977), pp. 57-71.

50. J. L. Camahort, E. H. Rennhack, and W. C. Coons, "Effects of Thermal Cycling Environment on Graphite Epoxy Composites," 78th Annual ASTM Meeting, ASTM-STP-602, ASTM, Philadelphia, Penn. (1975) pp. 37-66.

51. R. G. Spain, "Thermal Microcracking of Carbon Fiber/Resin Composites," Composites 2 (1), 33-37 (March 1971).

52. H. T. Hahn and R. Y. Kim, "Proof Testing of Composite Materials," J. Comp. Mat. 9, 297-311 (July 1975).

53. V. P. Mazzio and R. L. Mehan, Effects of Thermal Cycling on the Properties of Graphite-Epoxy Components, ASTM-STP-617, ASTM, Philadelphia, Penn. (1977) pp. 466-480.

54. W. D. Bascom, et al., "The Interlaminar Fracture of Organic Matrix Composites - Woven Reinforcements," The Enigma of the Eighties: Environment, Economics, Energy, Vol. 24, SAMPE, Azusa, Calif. (1979), pp. 1592-1598.

55. S. Hanagud, et al., "Comparative Evaluation of Woven Graphite-Epoxy Composites," 20th Structures Conference, AIAA (1979), p. 275.

56. S. Smith and R. C. Yee, A New Technique for the Characterization of Structural Material Under Dynamic Loading, Lockheed LMSC, Sunnyvale, Calif. (1979).

57. R. F. Gibson and R. Plunkett, "Dynamic Mechanical Behavior of Fiber-Reinforced Components: Measurement and Analysis," J. Comp. Mat. 10, 325 (1976).

58. R. D. Adams, et al., J. Comp. Mat. 7, 68 (1973).

59. C. C. Chamis, R. F. Lark, and J. H. Sinclair, "Effects of Moisture Profiles and Laminate Configuration on the Hygro Stress in Advanced Composites," Materials Synergisms, Vol. 10, SAMPE, Azusa, Calif. (1978), pp. 684-700.

60. D. H. Kaelble and P. J. Dynes, "Moisture Diffusion Analysis for Composite Microdamage," The Enigma of the Eighties: Environment, Economics, Energy, Vol. 24, SAMPE, Azusa, Calif. (1979), pp. 351-363.

61. D. F. Adams, "Temperature and Moisture Induced Stress at the Fiber/Matrix Interface in Various Composite Materials," The Enigma of the Eighties: Environment, Economics, Energy, Vol. 24, SAMPE, Azusa, Calif. (1979), pp. 1458-1469.

62. R. DeIasi and J. B. Whiteside, Effect of Moisture on Epoxy Resins and Composites, ASTM-STP-658, ASTM, Philadelphia, Penn. (1978), pp. 2-20.

63. T. Liber, I. M. Daniel, and C. C. Chamis, "The Effects of Thermal Cycling on Advanced Composite Angle Ply Laminates," Paper presented 30th SPI Reinforced Plastics Conference, Washington, D.C., 4-7 February 1975.

LABORATORY OPERATIONS

The Laboratory Operations of The Aerospace Corporation is conducting experimental and theoretical investigations necessary for the evaluation and application of scientific advances to new military concepts and systems. Versatility and flexibility have been developed to a high degree by the laboratory personnel in dealing with the many problems encountered in the Nation's rapidly developing space systems. Expertise in the latest scientific developments is vital to the accomplishment of tasks related to these problems. The laboratories that contribute to this research are:

Aerophysics Laboratory: Aerodynamics; fluid dynamics; plasmadynamics; chemical kinetics; engineering mechanics; flight dynamics; heat transfer; high-power gas lasers, continuous and pulsed, IR, visible, UV; laser physics; laser resonator optics; laser effects and countermeasures.

Chemistry and Physics Laboratory: Atmospheric reactions and optical backgrounds; radiative transfer and atmospheric transmission; thermal and state-specific reaction rates in rocket plumes; chemical thermodynamics and propulsion chemistry; laser isotope separation; chemistry and physics of particles; space environmental and contamination effects on spacecraft materials; lubrication; surface chemistry of insulators and conductors; cathode materials; sensor materials and sensor optics; applied laser spectroscopy; atomic frequency standards; pollution and toxic materials monitoring.

Electronics Research Laboratory: Electromagnetic theory and propagation phenomena; microwave and semiconductor devices and integrated circuits; quantum electronics, lasers, and electro-optics; communication sciences, applied electronics, superconducting and electronic device physics; millimeter-wave and far-infrared technology.

Materials Sciences Laboratory: Development of new materials; composite materials; graphite and ceramics; polymeric materials; weapons effects and hardened materials; materials for electronic devices; dimensionally stable materials; chemical and structural analyses; stress corrosion; fatigue of metals.

Space Sciences Laboratory: Atmospheric and ionospheric physics, radiation from the atmosphere, density and composition of the atmosphere, aurorae and airglow; magnetospheric physics, cosmic rays, generation and propagation of plasma waves in the magnetosphere; solar physics, x-ray astronomy; the effects of nuclear explosions, magnetic storms, and solar activity on the earth's atmosphere, ionosphere, and magnetosphere; the effects of optical, electromagnetic, and particulate radiations in space on space systems.